Pergamon

PII: S0038–092X(00)00027–X

Solar Energy Vol. 68, No. 4, pp. 361–370, 2000

0038-092X/00/$ - see front matter

www.elsevier.com/locate/solener

APPLICABILITY OF HIGHLY REFLECTIVE ALUMINIUM COIL FOR SOLAR CONCENTRATORS

THOMAS FEND*,†, GARY JORGENSEN** and HARALD KÜSTER***

*Deutsches Zentrum für Luft- und Raumfahrt eV., Solare Energietechnik, Linder Höhe, D-51147 Köln, Germany

**National Renewable Energy Laboratory, 1617 Cole Boulevard, Golden, CO 80401-3393, USA

***Alanod Aluminium-Veredelung GmbH, Egerstraße 12, D-58256 Ennepetal, Germany

Communicated by CLAES GRANQVIST

Abstract—Because of their manufacturing flexibility and their low costs, mirrors based on anodized or coated sheet aluminium are a promising alternative as primary or secondary concentrators in a number of solar energy applications. They offer solar weighted reflectances of 88–91%, good mechanical properties and are easy to recycle. However, problems occur due to their limited corrosion resistance. Therefore, prior to application, lifetime tests including outdoor and accelerated ageing tests are necessary to prove their optical durability in terms of achieving a 10-year service lifetime. In this study the optical properties of a number of different aluminized reflector materials after accelerated and outdoor exposure tests have been investigated. Optical testing has been performed by measuring the spectral hemispherical reflectance of exposed samples and calculating the solar weighted value. Additionally, specular reflectance has been measured with a simple mobile reflectometer. Materials involved are standard commercial anodized sheet aluminium with layers of different thicknesses and standard high specular aluminium with a metaloxide layer system plus an anti-oxidation polymer coating. Results show that optical degradation is strongly dependent on climatic conditions. Non-organic coatings involved are primarily attacked by humid climates with higher amounts of atmospheric pollution. Standard anodized materials withstand outdoor and accelerated weathering. However reflectance tends to become less specular, which limits their application in concentrating technologies. Finally, small scale application tests have been performed to demonstrate the applicability concerning handling and mechanical connection with support structures. By measuring power density in the focus of a test collector, minimum specular reflectance requirements for trough systems can be defined. © 2000 Published by Elsevier Science Ltd. All rights reserved.

1. INTRODUCTION

Until a few years ago highly reflective aluminized sheet materials were predominantly used as reflectors for lamps in office and industrial buildings. Because of their good mechanical properties and low cost compared to silvered glass mirrors, aluminized reflectors are finding applicability to high temperature solar concentrating technologies. Furthermore high reflectance aluminized sheet is already being successfully applied in low concentrating technologies like compound parabolic concentrator (CPC) troughs and daylightening.

In solar thermal technologies large collector areas are needed in order to achieve the intended levels of installed power. Assuming a solar-electric efficiency of about 15%, typical of the solar electricity generating system (SEGS) plants in the Californian Mojave desert (Cohen *et al.*, 1999), then for a 10 MW installation, typical of decentralized wind installations in Germany, $\sim 75\,000$ m^2 of reflective surface would be required. Because the reflector material cost is roughly half of the collector cost, a strong need for inexpensive solar mirrors is evident.

Although aluminized reflectors are cost effective, lightweight and mechanically beneficial, their optical durability in real-world applications was uncertain. In a common US–American–Spanish–German project between the public research organizations National Renewable Energy Laboratory (NREL), Centro de Investigaciones Energéticas Medioambientales y Tecnológicas (= Energy, Environment and Technology Investigation Center; CIEMAT) and Deutsches Zentrum für Luft- und Raumfahrt (= German Aerospace Center; DLR), new candidates of reflective materials are tested and assessed for their applicability in outdoor installations. This project was intended to support industrial efforts

†Author to whom correspondence should be addressed. Tel.: +49-2203-601-2101; fax: +49-2203-66900; e-mail: thomas.fend@dlr.de

in assessing and improving the properties of candidate solar mirrors, including highly reflective aluminium coil materials.

2. EXPERIMENTAL TESTING

2.1. Reflective materials testing

To demonstrate field service durability and to correlate degradation with accelerated test results, an 'Outdoor Exposure Test Program' was initiated by NREL in the US in 1994 (Wendelin and Jorgensen, 1994). In 1995 and 1996 the German Aerospace Center (DLR) and the Spanish Research Center CIEMAT joined the program and a co-operation was founded under the auspices of the International Energy Agency, Solar Power and Chemical Engineering Systems (IEA-Solar PACES) Subtask 3.3.2 '*Materials Development and Testing*'. This collaborative activity consists of outdoor testing including meteorological data monitoring, accelerated testing and optical measurements at regular intervals (Jorgensen *et al*., 1996). Experimental details are described in the next three sections.

2.1.1. Optical testing. To assess the optical performance and durability of candidate reflector materials, two methods of optical testing are performed. First, solar weighted hemispherical reflectance $\rho_{2\pi S}$ is calculated from the spectral hemispherical reflectance $\rho_{2\pi}(\lambda)$ according to ASTM Standard E903-82 (1993). The quantity $\rho_{2\pi}(\lambda)$ is measured in the wavelength range $250 < \lambda < 2500$ nm with Perkin-Elmer Lambda-series UV-VIS-NIR spectrometers equipped with integrating sphere attachments. Then a standard solar spectrum is used (ASTM Standard E891-87, 1993) to obtain *solar weighted* hemispherical reflectance values using the following formula:

$$\rho_{2\pi S} = \frac{\sum_{i=0}^{450} \rho_{2\pi}(\lambda_i) \cdot E(\lambda_i)}{\sum_{i=0}^{450} E(\lambda_i)}$$

$E(\lambda_i)$ denotes direct normal spectral irradiance at wavelength λ_i given in 5 nm steps ($\lambda_0 = 250$ nm, $\lambda_1 = 255$ nm, . . . , $\lambda_{450} = 2500$ nm). Agreement of measurements taken at the labs of the participating organizations was ensured by Round Robin Tests performed in 1995. The wavelength range 250 to 2500 nm covers ~98.5% of the total terrestrial solar power.

A second optical measurement is specular reflectance, *R*, as measured with a REFO3D reflectometer (manufactured by Dr. Lange, Berlin, Germany) according to the international standard ISO 7668 (1986). The instrument consists of a light source and housing with a lens that directs a parallel beam of light on to the surface under test and a receptor housing containing a lens, a receptor aperture and a photoelectric cell to receive the cone of reflected light. The measured signal is proportional to the reflected intensity integrated over the beam divergence angle defined by the instrument's aperture. It is a rectangular aperture with angles of 1.8° and 3.6°. Note that specular reflectance is not a unique physical property of the reflecting surface. It varies with the angle of measurement and with the aperture dimensions, which define the incident and the reflected beams. Furthermore the REFO3D reflectometer uses a lamp with a spectral intensity distribution which differs from the solar spectrum. Thus, the two values specular reflectance *R* and solar weighted hemispherical reflectance $\rho_{2\pi S}$ are not directly comparable. In this paper all data taken with the REFO3D reflectometer refer to incident angles of the source light on to the sample of 20°. Though not comparable with the solar weighted data, the REFO3D values provide important information about the applicability of candidate materials in concentrating technologies. Note that only materials with a thin coating on the reflective layer like anodized aluminium or silvered polymer films can be measured with this instrument.

More precise measurement methods as reported by Susemihl and Schissel (1987) and by Pettit (1977) are too expensive and too time consuming to be performed for large numbers of test samples.

2.1.2. Outdoor testing. Outdoor testing is currently performed at eight test-sites, six in the US and two in Europe. Geographic locations, average annual insolation, temperature and humidity data are shown in Table 1. Every test site consists of exposure racks, tilted at the latitude angle, and a meteorological station that records weather data including radiation values specified in the next section. Two of these sites are run in co-operation with public utilities: Arizona Public Service (APS) and Sacramento Municipal Utility District (SMUD) provide site support at Phoenix, AZ and Sacramento, CA, respectively. NREL (Golden), DLR (Köln) and the Plataforma Solar de Almería (PSA) operate test sites at their laboratory facilities. The Fort Davis site is run in co-operation with a group of utilities. The Dagget site is at the Solar Two plant, a joint undertaking between

Table 1. Meteorological conditions of presently available test sites

Location	Solar radiation (kWh/m^2 year)	Temperature (°C)	Relative humidity (%)
Köln (Germany)	694	10.5	78
Almería (Spain)	1805	18.5	67
Sacramento (CA, USA)	2000	16.0	66
Phoenix (AZ, USA)	2361	22.6	37
Fort Davis (TX, USA)	No long term data available		
Golden (CO, USA)	2000	10.2	52
Dagget (CA, USA)	2417	19.8	35
Miami (FL, USA)	1888	24.4	73

the US Department of Energy and a major consortium of utilities. Exposure at the Miami site is subcontracted to a commercial organization (South Florida Test Services).

At each test site the following meteorological quantities are measured: global insolation (total spectrum) at latitude angle, global ultraviolet insolation (295–395 nm) at latitude angle, global UV-B insolation (285–320 nm) at latitude angle, temperature, relative humidity, precipitation (rain, snow, ice), and wind (speed, direction). A complete description of the instruments used for meteorological monitoring is provided by Wendelin and Jorgensen (1994).

Usually three samples of each material type are exposed to receive statistically reliable results. Optical measurements are performed prior to exposure and after 6 months of exposure. Thereafter, regular measurements are repeated every 12 months. Data from all outdoor sites are collected at NREL. Within the SolarPACES agreement a report is in preparation that contains data for all exposure sites.

2.1.3. Accelerated testing. The results of the weather simulator tests presented in this study were performed by CIEMAT using an accelerated weathering test chamber equipped with 40 W fluorescent UV-B lamps and a condensation mechanism (QUV-Test-chamber, manufactured by Q-Panel Co., Bolton, UK). Tests were performed according to an American standard (ASTM Standard G53-95, 1995). This standard also specifies the intensity spectrum of the UV-B lamps, which show a peak emission at 313 nm. Test cycles consist of 4 h of UV exposure at 60°C and 4 h of vapour condensation exposure at 50°C. The average distance sample–light source is 55 mm. The accelerating effect of this instrument is due to its more intense radiation in the UV-range compared to the solar spectrum. Care must be taken when using such a device to prevent unrealistic degradation caused by irradiance at wavelengths below the terrestrial cut-off at about 300 nm.

In addition, accelerated weathering was performed at NREL with an Atlas Ci65 WeatherOmeter (WOM) and an Heraeus (now Atlas) XENOTEST 1200 LM. These chambers allow control of temperature and ambient humidity and use a xenon-arc light source with filters to give a close match to a terrestrial air mass 1.5 solar spectrum at an average distance of the samples from the light source. The chambers have been operated at 60°C and 75% relative humidity.

2.2. Small scale application tests

2.2.1. Test of an aluminium coil reflector as a HELIOMAN[1] collector-element. The applicability of aluminium coil for use as a parabolic trough collector mirror was tested by bonding a highly specular sheet aluminium material (Miro 2, a product of Alanod) onto the existing thick glass of a HELIOMAN type concentrator. The energy striking the absorber tube was measured with a HYCAL circular foil radiometer, which was installed in the tube (Fig. 1). The experimental set-up for these measurements was described in more detail in a previous paper (Fend and Wenzel, 1999).

2.2.2. Test of an aluminium coil as a HELIOMAN end-reflector collector-element. Using the same equipment described in the last paragraph the performance of an additional end-reflector, installed at one side of the test collector, was investigated. The radiometer was installed 15 cm from the end of the trough. Investigating various angles of incidence of the solar radiation, the effect of the end-reflector on the distribution of the concentrated flux in the focal area could be observed.

2.2.3. Almería LS-3 end-reflector tests. As described in more detail by Fend *et al*. (1999), a 6.4-m^2 end-reflector made out of coated sheet aluminium (Miro 2) was installed at the DISS-Reference test loop at the PSA in Almería (Fig.

[1]A collector module built by the German company MAN in the early 1980s (Meinecke and Bohn, 1994).

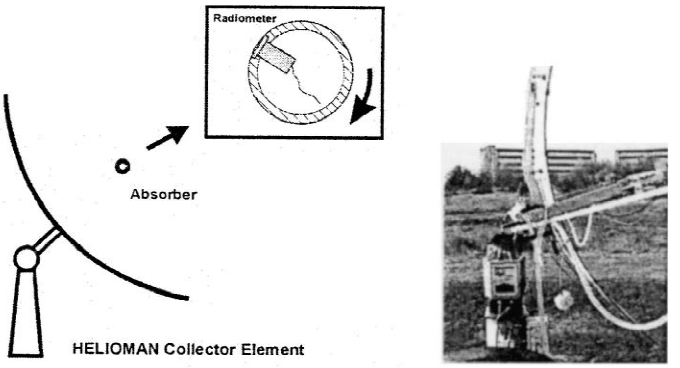

Fig. 1. Schematic view and photograph of the equipment for measuring power densities in the focus of a HELIOMAN type parabolic trough collector.

2). Efficiency tests comparing the performance with and without this additional reflector were carried out at the PSA in June 1998. The objectives of this test were (1) to show the efficiency increase that can be reached with an additional end reflector, and (2) to demonstrate the large-scale applicability of coated aluminium as a solar reflector material. The test loop consists of a 50-m LS-3 parabolic trough collector with an aperture width of 5.70 m, a collector type also used in later generation SEGS-plants (Hertlein *et al.*, 1991). The additional end reflector was designed as a modular frame system, which may easily be installed in existing north–south aligned troughs. It consists of six single modules made out of aluminium frames. Onto these frames, sheet aluminium facets were glued to completely cover the end of the trough. Each module was adjusted with a laser system, simulating solar radiation striking the trough or the end-reflector facets with various incident angles. The efficiency, η, of the loop as an effect of the additional mirror was calculated from mass-flow and temperature data (T_{out} and T_{in}) of the heat transfer fluid as well as from direct normal incident solar radiation data (I) using:

$$\eta = \frac{\dot{m} \cdot C_{\mathrm{p}} \cdot (T_{\mathrm{out}} - T_{\mathrm{in}})}{I \cdot A},$$

where A denotes the aperture area of the collector

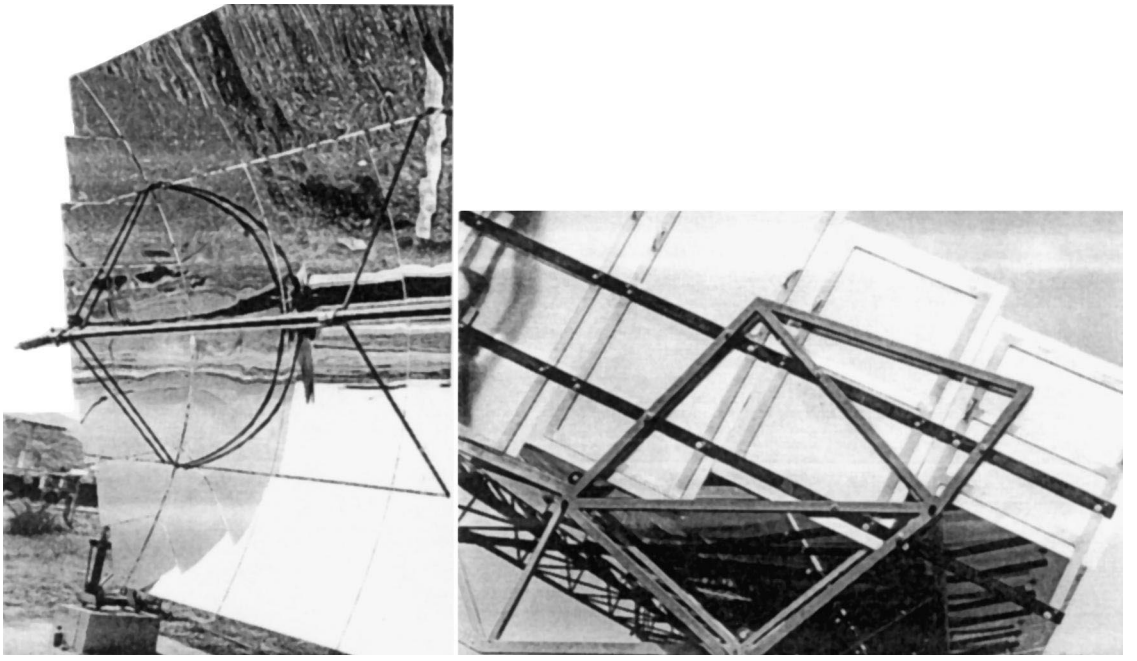

Fig. 2. Front and backside views of the additional end-reflector designed and installed at the LS-3 collector of the DISS-reference test loop at the PSA.

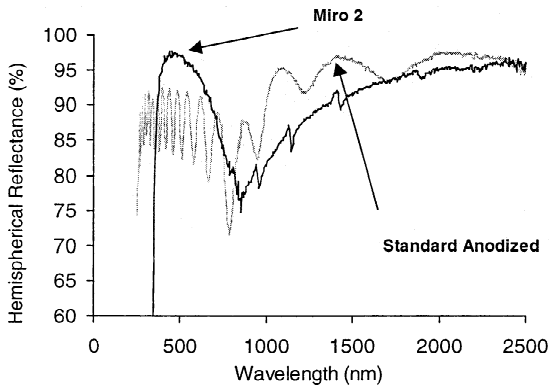

Fig. 3. Spectral hemispherical reflectance $\rho_{2\pi}(\lambda)$ of a standard anodized aluminium material compared to the reflectance of Miro 2.

and C_p the specific heat of the heat transfer fluid. To characterize the optical properties of the collector, the solar-to-thermal efficiency η is replaced by the relative efficiency η/η_0 with η_0 denoting the collector efficiency for $\theta = 0°$ incident angle of the solar radiation.

3. SAMPLE PREPARATION OF PVD-COATED ALUMINIUM-REFLECTOR MATERIAL

Four types of highly reflective aluminium coil material were tested. The first two were standard anodized aluminium materials. One standard material is produced on a coil and will be denoted within this text as STAAC (standard anodized aluminium coilcoated) and one by anodizing single pieces, further denoted as STAAP (standard anodized aluminium coated piece-by-piece). These were compared with two physical vapour deposition (PVD)-coated types of aluminized sheets Miro 2 and Miro 2+. Miro 2 is the trade name of the material, which is available on the market and Miro 2+ is the same material but equipped with an additional protective lacquer.

The PVD-coated material is especially appealing because of its enhanced reflectivity in the visible spectrum (Fig. 3). This results in an increase of the solar weighted hemispherical reflectance $\rho_{2\pi S}$ of about 2–3%. This material is processed by an inline vacuum coater. Standard anodized coils can serve as a substrate onto which an optical three-layer coating is deposited.

First, an opaque pure aluminium layer is sputtered (DC Magnetron sputtering at 10^{-3} mbar). This serves as a spectrally broad reflecting surface with a $\rho_{2\pi S}$ of about 89%. It is known that a pure aluminium surface is very sensitive to mechanical and chemical attack and has to be protected. For head lights in cars and other low-cost applications often a SiO_2-layer is used for protection. Such a coating can be deposited either by plasma enhanced chemical vapour deposition (PECVD) of hexamethyldisiloxan (HMDSO) or by thermal reactive evaporation of SiO or other suboxides. Deposition of an SiO_x overcoat will decrease reflectance.

To enhance the reflectance in the visible spectrum, a second high refracting dielectric layer can be added by means of reactive electron beam evaporation. This composition makes use of the constructive interference effects from three interfaces and two transparent layers. Using SiO_2 (low refractive index $n_L = 1.44$ at 550 nm) and TiO_2 (high refractive index $n_H = 2.25$ at 550 nm) reflectance in the visible spectrum can be increased significantly. A schematic drawing of a Miro 2 and a Miro 2+ cross-section is provided in Fig. 4.

Both layers can be produced by different means, but an industrial competitive process can only be conducted with reactive e-beam evaporation. The structure of the reactively processed SiO_2- and TiO_2-films is known to be columnar and porous. For interior applications of PVD-coated aluminium, there are no problems with these layers. The mechanical and chemical resistance are very good and fulfil customers requirements (mostly manufactures of louvers).

Outdoor durability is a much tougher requirement. One year outdoor weathering in Köln,

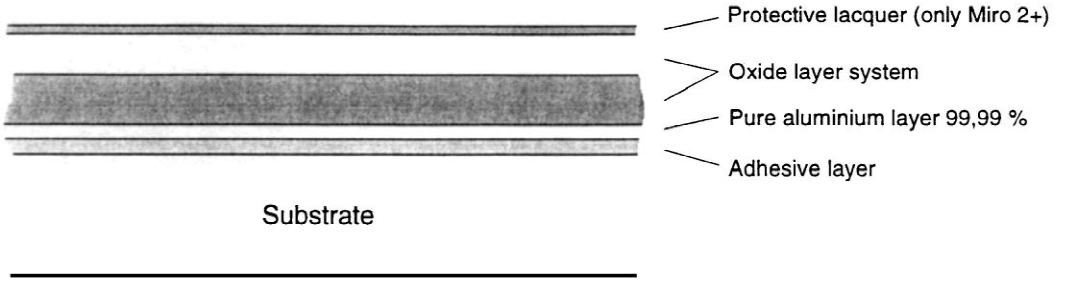

Fig. 4. Schematic view of the structure of Miro 2 and Miro 2+.

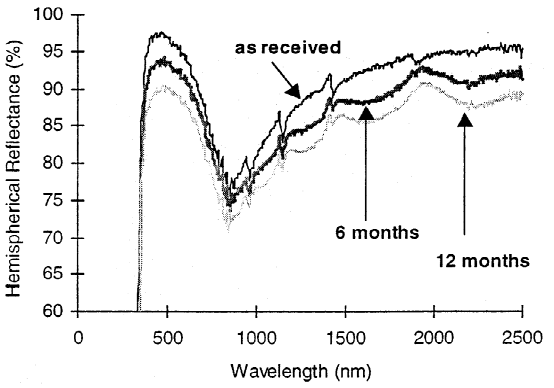

Fig. 5. Spectral hemispherical reflectance $\rho_{2\pi}(\lambda)$ of an aluminium material with additional PVD oxide layers (Miro 2) after different exposure times.

Germany at the DLR test facility of Miro 2 resulted in a decrease in solar weighted hemispherical reflectance $\rho_{2\pi S}$ from 88.6% to 82.6% (Fig. 5). Microscopic investigation showed pit corrosion taking place at the outermost interface of the sputtered aluminium layer (Fig. 6). Apparently the porosity of SiO_2 and TiO_2 is too large to prevent penetration of humidity and corrosive salts through the coating and to the sensitive Al/SiO_2-interface.

The solution to this problem is a protective lacquer. This lacquer has to have a very high solar transmittance, a very good stability against ultraviolet radiation, good adhesion to the oxide coating, and only a negligible effect on $\rho_{2\pi S}$. In the text, this additionally coated material is denoted as Miro 2+. Alanod is working on further improvements of this material.

4. RESULTS AND DISCUSSION

4.1. Outdoor and accelerated exposure tests

Among the wide variety of reflective materials being tested within the collaborative SolarPACES activity, four different types of reflectors based on anodized aluminium have been investigated in more detail to be compared in this paper. In contrast to excellent outdoor performance of glass materials silvered at the backside and of aluminized polymer mirrors (Fend *et al.*, 1996), most types of front surface aluminium reflectors exhibit degradation during exposure testing. Figs. 7 and 8 summarize the outdoor performance of the investigated anodized aluminium mirror candidates. Reflectance measurements are carried out before and after sample cleaning. Thus, at every time two values are plotted in the graph. Standard anodized materials (STAAC and STAAP) show a slight decrease in hemispherical reflectance but a severe decrease in specular reflectance after outdoor exposure, which makes them unapplicable for concentrating technologies such as parabolic troughs. In both cases degradation is most rapid at the Köln test site, indicating that damage is strongly dependent on climatic conditions. Also the reflection enhanced material Miro 2 shows degradation due to corrosion, being most rapid in Köln. However, the additional polymer coating (Miro 2+) stopped corrosive attack throughout the duration of the experiment.

In addition to outdoor experiments, accelerated weathering has been carried out in test chambers described in Section 2.1.3. Results are shown in Fig. 9. The degradation is limited to 1–2% during a 12-month exposure time, which is much lower than after outdoor exposure at the Köln site. Apparently, atmospheric and rain water pollution, which is not simulated in the accelerated weathering chambers, limits the useful lifetime of these materials. Tests with a more severe simulation of such climates, the salt spray test, showed no visible and optical degradation for the Miro 2+ ($\rho_{2\pi S} = 89.3\%$ after 1000 h). For testing the UV-stability of the additional polymer coating of the Miro 2+ material, QUV tests have been carried

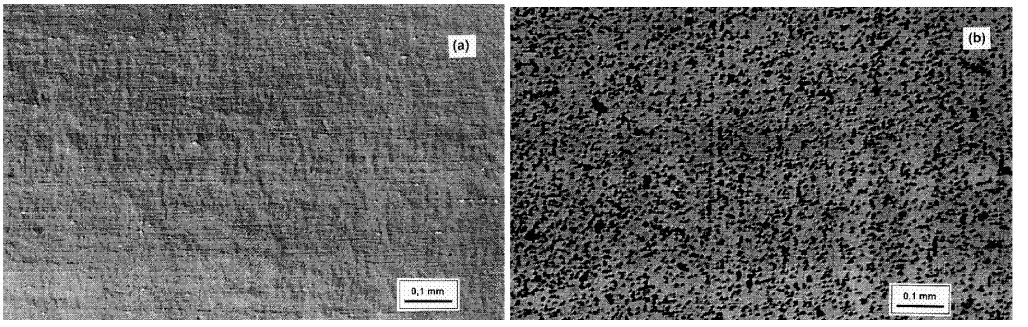

Fig. 6. Optical micrographs of new (a) and exposed (b) Miro 2 material.

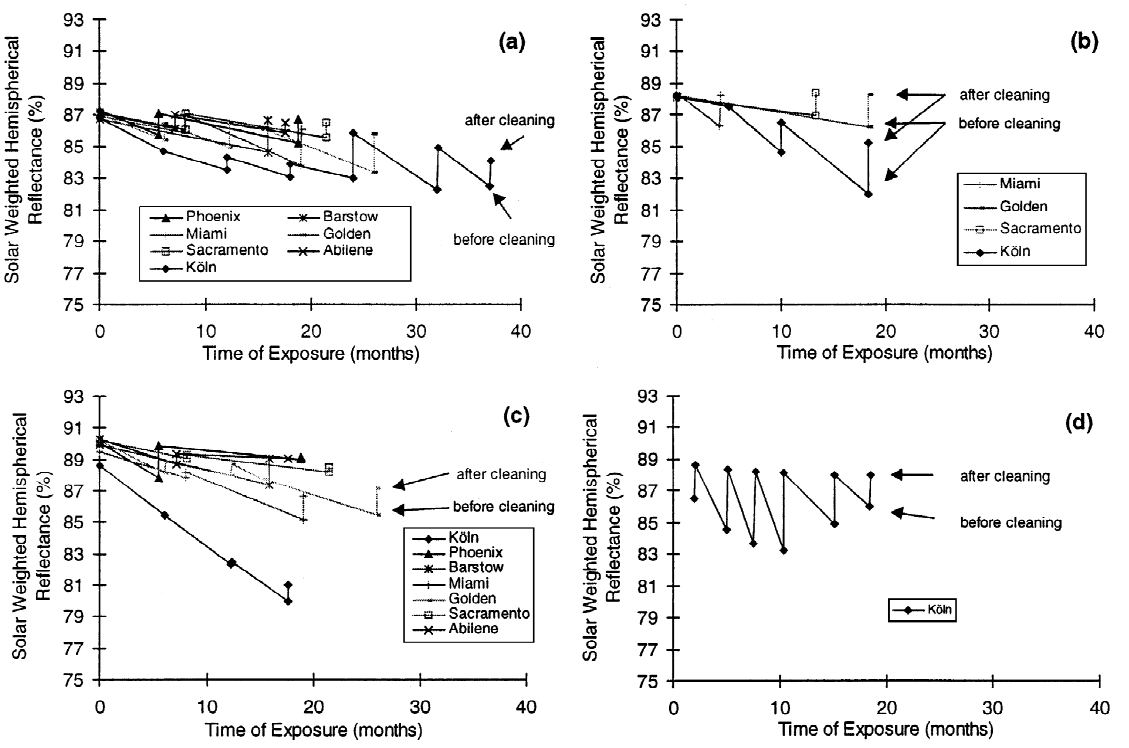

Fig. 7. Solar weighted hemispherical reflectance $\rho_{2\pi S}$ of the four investigated materials as a function of outdoor exposure time at different test sites: (a) STAAP, (b) STAAC, (c) Miro 2 and (d) Miro 2+.

out. No significant decrease of $\rho_{2\pi S}$ was observed after 1400 h exposure.

4.2. Performance tests of Miro 2 as a HELIOMAN-facet

Exposure tests and optical reflectance measurements are a necessary precondition for the selection of collector material candidates. However, additional problems may occur during manufacturing of the collector, possibly due to geometrical errors of the mirrors. Furthermore, the measured specular reflectance properties of the materials investigated are not guaranteed to meet the requirements in concentrating technologies.

To test the applicability of an aluminized coil reflector in a real-world solar concentrator application, the test loop described in Section 2.2.1 was equipped with a Miro 2 mirror glued onto the original HELIOMAN collector element. Fig. 10 shows the flux density at the surface of an absorber tube for the aluminium material compared with the original backside-silvered thick (4 mm) glass. The integrated flux over the total circumference of the tube was 13% less for the aluminium mirror. However, the difference in

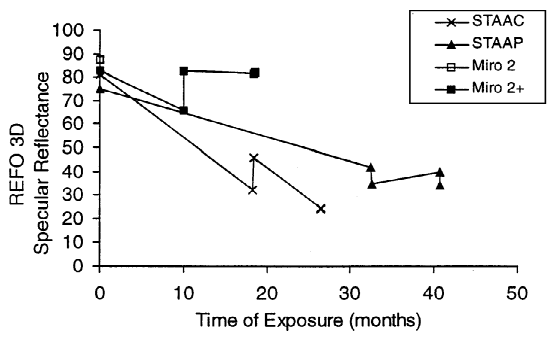

Fig. 8. Specular reflectance properties of the investigated materials as a function of outdoor exposure time at the Köln test site.

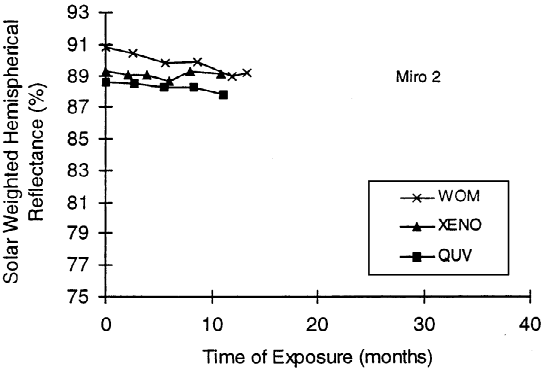

Fig. 9. Solar weighted hemispherical reflectance $\rho_{2\pi S}$ of Miro 2 after different methods of accelerated ageing.

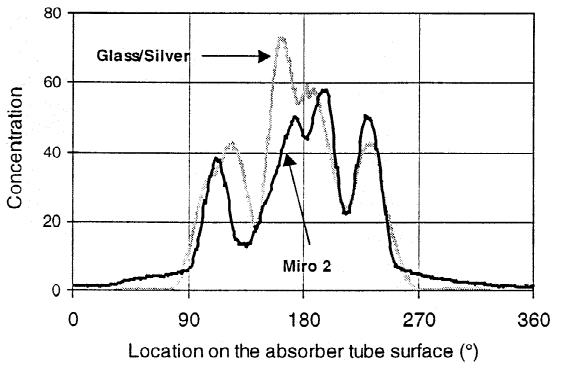

Fig. 10. Optical flux density distribution on the surface of the absorber tube of a parabolic trough from the HELIOMAN-type collector (averages: silvered glass: 18.3; aluminium: 16.3).

solar weighted hemispherical reflectance is only about 5%. Thus, the specular properties of the Miro 2 reflector resulted in the additional optical losses. The angular scattering distribution shows high scattering especially in the ranges between 30°–80° and 260°–320°. Despite the measured difference in performance, coated sheet aluminium is an alternative because of its low price and good mechanical properties compared to silvered glass.

4.3. Performance tests of Miro 2 as a HELIOMAN end-reflector element

As a further application test of Miro 2, its performance as a HELIOMAN-end-reflector element was tested, using the equipment described in Section 2.2.2. Results are shown in Fig. 11. Plotted points result from radiometer power density measurements of the absorber tube, which were integrated over the circumference of the absorber tube. Each point represents the ratio of the measurement with and without the end-reflector. The *x*-axis represents the direction of the line

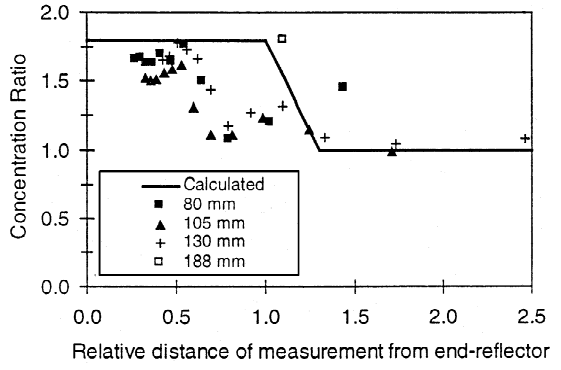

Fig. 11. Summary of flux measurements at different positions on the absorber tube and for different incident angles.

focus with 0 indicating the position of the end reflector. The theoretical curve shown in the plot is the result of a model that assumes an ideally reflecting mirror. The model as well as additional experimental details are described in a previous paper (Fend *et al.*, 1999).

Data points result from measurements at different distances of the radiometer position from the end reflector. At each position the incident angle was varied, so a greater variety of different points within the end loss zone could be achieved. The majority of the data points are below the theoretical curve. This is mainly caused by the limited specular properties of the end reflector's surface. Radiation, which is first reflected by the aluminium and secondly by the glass/silver mirror, undergoes greater scattering than if the order of the reflective surfaces was switched. The optical losses of the collector increase with increasing incident angle. This effect is even more pronounced when a twofold reflection occurs, as in the case of an end reflector. Furthermore, the sheet aluminium in this case was glued onto a stainless steel frame and a slight curvature occurred, which was probably caused by the differences in thermal expansion of these two materials. This curvature resulted in light spillage during characterization of the end-reflector. However, the measurements show that a significant increase in efficiency may be achieved using an additional end-reflector. Consequently, a test on a larger-scale unit was performed, which is described in the next section.

4.4. Performance tests of Miro 2 as an LS-3 collector end-reflector element

Fig. 12 summarizes the efficiency tests carried out with an LS-3 collector test loop at the PSA. Efficiency is plotted as a function of the incident angle of the solar radiation into the trough. In East–West aligned one-axis tracked parabolic trough collector systems like the LS-3 test collector at the PSA the incident angle θ of the solar radiation becomes zero at solar noon. Due to non-zero incident angles at all other times, efficiency as a function of θ theoretically decreases proportional to cos θ (cosine losses). Practically, as can be seen for the 'no End Reflector' curve in Fig. 12, the decrease is larger because of optical losses that increase with increasing incident angle. Optical losses are higher for greater incident angles mainly because of the longer distance from the point of reflection on the reflector to the point of absorption on the heat collecting element. Scattering losses between the reflector and the

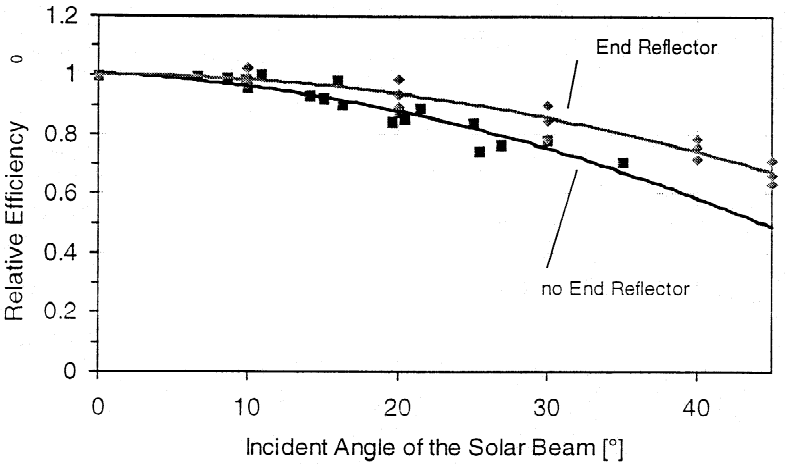

Fig. 12. Relative efficiency as a function of incident angle of the LS-3 collector at the DISS-Reference loop of the PSA comparing the performance of an additional end-reflector with the original configuration.

absorber are accentuated by the longer optical path. On the other hand, for non-zero incident angles the end reflector collects radiation that would otherwise have missed the absorber. The effect increases with increasing incident angle, so it compensates part of the cosine losses. The efficiency can be increased significantly by the addition of an end reflector ('End Reflector' curve in Fig. 12). Using the efficiency data shown in Fig. 12, 'clear sky' annual efficiencies may be roughly estimated for north–south aligned troughs of the same length. Assuming the geographical data of Southern Spain (35° northern latitude) an increase of the annual efficiency of 3% is predicted.

5. CONCLUSIONS

Of the materials investigated, highly specular aluminium has an excellent chance to meet the requirements for medium-concentrating technologies like parabolic troughs. For applications in humid climates, an additional polymer coating is necessary for optical durability. Standard anodized materials show satisfactory hemispherical reflectance properties after outdoor and accelerated exposure. However, their specular reflectance properties disqualify them for application in troughs or heliostats. Accelerated test methods provide only a limited criterion to assess the applicability of aluminized reflector materials in practical use, because the degradation process is not completely understood. Further improvements of the currently used accelerated test methods are necessary. Mini-plant tests show that the specular properties of the enhanced reflectance aluminized material are good enough for application in parabolic troughs.

NOMENCLATURE

A	aperture area of the collector (m^2)
λ	optical wavelength (nm)
$E(\lambda_i)$	direct normal spectral irradiance at wavelength λ_i ($W/(m^2$ nm))
$\rho_{2\pi}(\lambda)$	spectral hemispherical reflectance (%)
$\rho_{2\pi S}$	solar weighted hemispherical reflectance (%)
R	specular reflectance measured with the REFO3D spectrometer (arbitrary units)
η	solar-to-thermal efficiency (%)
η_0	solar-to-thermal efficiency for 0° incident angle θ (%)
I	direct normal incident solar radiation (W/m^2)
T_{in}	inlet temperature of the heat transfer medium (°C)
T_{out}	outlet temperature of the heat transfer medium (°C)
C_p	specific heat of the heat transfer medium (J/kg K)
$\dot{m}$	mass flow of the heat transfer medium (kg/s)
n_L, n_H	refractive indices of light reflectance improving coating system

REFERENCES

ASTM Standard E903-82 (1993) Standard test method for solar absorptance reflectance, transmittance of materials using integrating spheres. In Annual Book of ASTM Standards 1993, Vol. 12.02, p. 512, American Society for Testing and Materials, Philadelphia, PA.

ASTM Standard E891-87 (1993) Standard tables for terrestrial direct normal solar spectral irradiance for air mass 1.5. In Annual Book of ASTM Standards 1993, Vol. 12.02, p. 481, American Society for Testing and Materials, Philadelphia, PA.

ASTM Standard G53-95 (1995) Operating light- and water-exposure apparatus (fluorescent UV-condensation type) for exposure of non-metallic materials. In Annual Book of ASTM Standards 1995, American Society for Testing and Materials, Philadelphia, PA.

Cohen G. E., Kearney D. W. and Price H. W. (1999) Performance history and future costs of parabolic trough solar electric systems. In *Proceedings of the 9th International Symp.-Solar PACES-Solar Thermal Concentrating Technologies, Les Ulis Cedex A, France*, Flamant G. and Ferrière A. et al. (Eds.), p. 563.

Fend T., León J., Böhmer M., Binner P., Deidewig F. and Kemme R. (1999) Development and test of an end reflector for parabolic trough collectors. In *Proceedings of the 9th International Symp.-Solar PACES-Solar Thermal Concentrating Technologies, Les Ulis Cedex A, France*, Flamant G. and Ferrière A. (Eds.), p. 563.

Fend T., Sánchez M., Morales A., Rietbrock P. and Böhmer M. (1996) Optical properties and exposure tests of solar reflective materials. In *Proceedings Eurosun '96*, Goetzberger A. and Luther J. (Eds.), p. 510, DGS-Sonnenenergie Verlags-GmbH, München, Germany.

Fend T. and Wenzel K. (1999) Optical flux measurements in the focal area of a parabolic trough concentrator. In *Proceedings of the 9th International Symp.-Solar PACES-Solar Thermal Concentrating Technologies, Les Ulis Cedex A, France*, Flamant G. and Ferrière A. (Eds.), p. 605.

Hertlein H. P., Klaiss H. and Nitsch J. (1991) Cost analysis of solar power plants. In *Solar Power Plants*, Winter C.-J., Sizman R. L. and Vant-Hull L. L. (Eds.), p. 374, Springer Verlag, Berlin.

ISO 7668 (1986). In 1st edn, Anodized Aluminium and Aluminium Alloys — Measurement of Specular Reflectance and Specular Gloss at angles of 20°, 45°, 60° or 85°, 1986-10-15.

Jorgensen G., Böhmer M., Fend T. and Sánchez M. (1996) International collaborative testing of solar reflectors. In *Proceedings of the 8th International SolarPACES Symposium, Köln, Germany*, Becker M. and Böhmer M. (Eds.), p. 443.

Meinecke W. and Bohn M. (1994). In *Solar Energy Concentrating Systems*, Becker M. and Gupta B. (Eds.), p. 24, C.F. Miller Verlag, Heidelberg.

Pettit R. B. (1977) Characterisation of the reflected beam profile of solar mirror materials. *Solar Energy* **19**, 733.

Susemihl I. and Schissel P. (1987) Specular reflectance properties of silvered polymer materials. *Solar Energy Mater*. **16**, 403.

Wendelin T. and Jorgensen G. (1994). *An Outdoor Exposure Testing Program for Optical Materials Used in Solar Thermal Electric Technologies*, NREL, Golden, CO, TP-471-5865.